

Evidence for free precession in a pulsar

I. H. Stairs, A. G. Lyne & S. L. Shemar

University of Manchester, Jodrell Bank Observatory, Macclesfield, SK11 9DL, UK

Pulsars are rotating neutron stars that produce lighthouse-like beams of radio emission from their magnetic poles. The observed pulse of emission enables their rotation rates to be measured with great precision. For some young pulsars, this provides a means of studying the interior structure of neutron stars. Most pulsars have stable pulse shapes, and slow down steadily (for example, see ref. 20). Here we report the discovery of long-term, highly periodic and correlated variations in both the pulse shape and the rate of slow-down of the pulsar PSR B1828–11. The variations are best described as harmonically related sinusoids, with periods of approximately 1,000, 500 and 250 days, probably resulting from precession of the spin axis caused by an asymmetry in the shape of the pulsar. This is difficult to understand theoretically, because torque-free precession of a solitary pulsar should be damped out by the vortices in its superfluid interior^{1,2}.

PSR B1828–11 (PSR J1830–1059) is a young pulsar which is observed on about 30 occasions each year using the 76-m Lovell radio telescope at Jodrell Bank; the complete data set spans nearly 13 years. The integrated pulse profile is not stable. It consists of a wide component with a central, narrower peak which varies in intensity on timescales of several months. For each observation, we can determine a ‘shape parameter’ *S*, which describes the pulse shape, as well as a pulse time-of-arrival (TOA).

Pulsar timing analysis consists of fitting a model of the pulsar rotation to the observed TOAs, and examining the residuals, which are the differences between the TOAs and the best-fit model. If the timing model is correct, the residuals should be gaussianly distributed about zero. The timing residuals for PSR B1828–11 are shown in Fig. 1. More than four cycles of an evolving double-peaked pattern with period of about 1,000 days can be seen. In order to study the variations in more detail, the timing residuals, the rotation period *P*, the period derivative \dot{P} and the shape parameter *S* have been calculated for the most recent 2,000 days (Fig. 2). In particular,

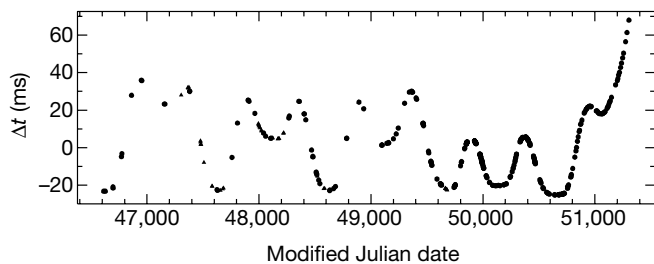


Figure 1 Post-fit timing residuals Δt for PSR B1828–11 after fitting for the spin-down parameters given in Table 1. Each point represents an observation of roughly 30 minutes’ duration at a frequency around 1,400 MHz (circles) or 1,600 MHz (triangles). Individual profiles are described by a linear combination of two extreme standard profiles, one wide, one narrow. An iterative frequency-domain routine was used to determine the relative strengths of the standard profiles required to synthesize the daily profiles. This provides a ‘shape parameter’, $S = \frac{A_N}{A_N + A_W}$, where A_N and A_W are the fitted heights of the narrower and wider standard profiles respectively, so that $S \approx 1$ for the narrowest pulses and $S \approx 0$ for wider ones. The pulse times-of-arrival (TOAs) are also derived from this shape-fitting procedure; the errors in the TOAs are limited by random noise to about 0.2 ms.

Table 1 Measured and derived parameters of PSR B1828–11

Period, <i>P</i>	405.039883158(8) ms
Period derivative, \dot{P}	$60.03243(9) \times 10^{-15}$
Period second derivative, \ddot{P}	$-1.70(3) \times 10^{-25} \text{ s}^{-1}$
Epoch of period	MJD 48958
Right ascension, α (J2000)	18 h 30 min 47.583(7) s
Declination, δ (J2000)	$-10^\circ 59' 29.33(12)''$
Dispersion measure, DM	$159.7(10) \text{ cm}^{-3} \text{ pc}$
Magnetic field, <i>B</i>	$5.0 \times 10^{12} \text{ G}$
Characteristic age, τ_c	0.11 Myr

Uncertainties in least-significant digits are given by numbers in parentheses. Timing parameters were determined using the TEMPO software package (<http://pulsar.princeton.edu/tempo>) and the JPL DE200 planetary ephemeris. The adopted dispersion measure was obtained from same-epoch 1,400-MHz and 600-MHz observations. The pulsar position was determined from timing measurements and refined using interferometric observations with the Very Large Array (VLA). The period first and second derivatives were fitted after whitening the timing residuals by removing a series of high-frequency sinusoids. The choice of the period second derivative, in particular, is therefore somewhat arbitrary, and may affect attempts to model the longest-term variations in the timing residuals.

the variations in pulse shape (*S*) are highly correlated with the changes in the period derivative \dot{P} . A spectral analysis of the four time sequences (Fig. 3) shows that all contain harmonically-related periodicities of approximately 1,000, 500 and 250 days.

We consider in turn whether these periodic phenomena originate outside the pulsar in a planetary system, in the neutron superfluid within the star, or in the precession of the star. The harmonically-related period variations alone would suggest a Doppler effect due to a system of gravitationally interacting planets orbiting the pulsar³, as observed for the millisecond pulsar PSR B1257+12 (refs 4–6). However, it does not seem credible that the pulse profile

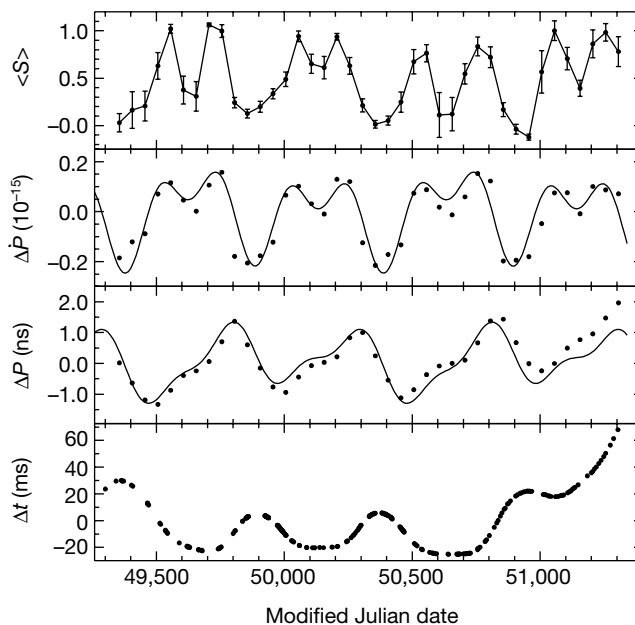


Figure 2 Variations in rotation and pulse shape in PSR B1828–11. The displayed time series are the residuals in arrival time Δt , and period ΔP and derivative $\Delta \dot{P}$, relative to the spin-down model given in Table 1, and the mean pulse shape parameter $\langle S \rangle$ for the most recent 2,000 days, where the observations are most closely spaced. The period residual, ΔP , is the local value of the slope of Δt , and $\Delta \dot{P}$ is the second derivative. The three series ΔP , $\Delta \dot{P}$ and $\langle S \rangle$ were calculated over time intervals of 100 days which overlapped by 50 days. There is, within the uncertainties in $\langle S \rangle$, a clear similarity in form between the variations in $\langle S \rangle$ and in $\Delta \dot{P}$, although this is not obvious from the variations in period or from the observed timing residuals themselves. These periodic patterns continue back through the entire 13-year data set. The solid curves indicate the predictions of a fit of three harmonically-related sinusoids to ΔP ; the fundamental period is $1,009 \pm 8$ days. In addition to modelling ΔP , these fitted parameters, as expected, yield a good representation of $\Delta \dot{P}$.

variations are caused by a magnetospheric interaction similar to that between Jupiter and Io (for example, see ref. 7), as this would require at least two of these planets to interact with the pulsar magnetosphere over distances comparable to the size of the Earth's orbit. Timing noise (for example, see ref. 8), believed to be due to random movements of the fluid within the pulsar, could not produce the sustained and regular pattern which we observe. A Tkachenko oscillation⁹ in the interior superfluid might have a period of the order of several hundred days, but provides no explanation for the variations in pulse shape.

The close relationship between the periodic changes in the beam shape and the rate of spin-down is simply explained by precession of the neutron star spin axis (for example, see ref. 10). This effect is rarely observed in celestial bodies, but will occur if the star is deformed so that its spin axis is not aligned with its angular momentum vector. This would cause cyclic changes, possibly with harmonics, in the inclination angle α between the spin and magnetic axes. The result will be periodic variations in pulse-profile morphology as the line-of-sight to the Earth passes through different cross-sections of the pulsar's radiation beam, and corresponding changes in the spin-down torque acting on the pulsar. Within the context of the rotating magnetic dipole model, the slow-down rate and the magnetic inclination angle are related by $\dot{P} = 8\pi^2 m^2 \sin^2 \alpha / (3c^3 I P)$, where c is the speed of light, I the moment of inertia and m the dipolar magnetic moment of the

neutron star. The observed 0.7% variation in \dot{P} therefore implies a fractional change of similar magnitude in $\sin^2 \alpha$, or a variation in α of 0.3° for $\alpha \approx 60^\circ$. That is roughly one-tenth of the observed profile width of about 3° , and approximately the same magnitude as the observed change in width. That the shape changes are likely to be due to precession is supported by the fact that the only two other pulsars with well-measured long-term profile shape changes are the double-neutron-star binaries PSRs B1913+16 and B1534+12, which are undergoing precession due to general-relativistic spin-orbit coupling^{11,12}. PSR B1828-11 is somewhat different from these two pulsars in that it is solitary, and hence its precession cannot be influenced by another body. Although there have been suggestions¹³⁻¹⁵ that free precession might be the cause of possibly correlated timing behaviour and profile shape changes in other isolated radio pulsars, none but PSR B1828-11 shows strongly periodic variation in either pulse shape or rotation, let alone both. For instance, in PSR B1642-03 (ref. 13), the variation in shape is only marginally significant, and is not convincingly correlated with the aperiodic timing variations. Another family of neutron stars, the anomalous X-ray pulsars, are known to display 'wobblers' in their slowdown rates (for example, ref. 16); perhaps free precession could account for these variations, making it unnecessary to invoke the magnetar-strength magnetic fields required by the 'radiative precession' theory¹⁷. Further observations of all classes of neutron stars may therefore help to shed light on the physics involved in the precession indicated by the behaviour of PSR B1828-11.

Theoretical studies of the neutron-star interior present a difficulty here. The rotation of the superfluid, which accounts for a large proportion of the moment of inertia of the star, is contained in an array of vortices. The occurrence of and recovery from the starquakes known as glitches have been successfully described by models in which vortices pinned to the stellar crust become unpinned during a glitch¹⁸. However, the vortex pinning, even if it is imperfect, will damp out free (untorqued) precession on timescales of several hundred precession periods (see refs 1 and 2). Nevertheless, in light of the clearly periodic behaviour of the timing parameters and profile shape of PSR B1828-11, a model will have to be devised which allows for some amount of vortex pinning as well as precession. Perhaps the key to understanding will lie in how the vortex array, whether partly or wholly pinned, responds to a variable external electromagnetic torque such as that which a precession would apply. In this case, the precession may be long-lived but perhaps not perfectly regular. □

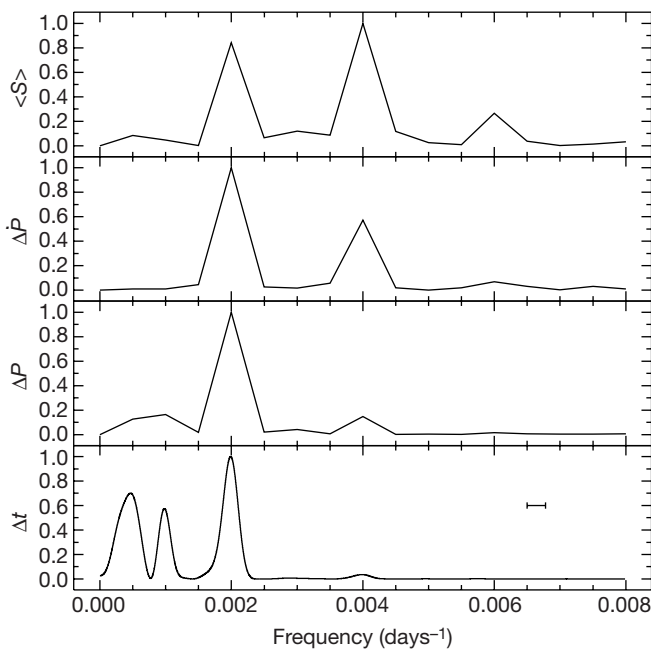


Figure 3 Harmonically related spectral features in the rotation and pulse shape of PSR B1828-11. The panels show the spectral power of the residuals Δt , ΔP , $\Delta \dot{P}$ and the mean pulse shape parameter $\langle S \rangle$. The normalizations are arbitrary. We used a one-dimensional CLEAN algorithm (for example, see ref. 19) for the timing residuals because of the uneven sampling within that data set; the horizontal bar indicates the full width of the smoothing function applied to the timing residual spectrum by this algorithm, and indicates that most of the spectral features are unresolved. The spectra exhibit harmonically related periodicities of approximately 1,000, 500 and 250 days, and confirm that the variations in shape and rotation are related. There is also a strong indication of the presence of a further harmonically related periodicity of approximately 167 days. The relative strengths of the harmonic components in the lower three plots change as expected from successive differentiation of the sinusoidal components of the timing residuals. We note that there is a good chance that the apparent power at around $1/2,000$ days in the lowest plot could be due primarily to timing noise in this young pulsar; for this reason we do not include this periodicity in the discussion in the text.

Received 1 September 1999; accepted 22 May 2000.

- Shaham, J. Free precession of neutron stars: role of possible vortex pinning. *Astrophys. J.* **214**, 251-260 (1977).
- Sedrakian, A., Wasserman, I. & Cordes, J. M. Precession of isolated neutron stars. I. Effects of imperfect pinning. *Astrophys. J.* **524**, 341-460 (1999).
- Bailes, M., Lyne, A. G. & Shemar, S. L. in *Planets Around Pulsars* (eds Phillips, J. A., Thorsett, S. E. & Kulkarni, S. R.) 19-30 (Astronomical Society of the Pacific Conference Series, San Francisco, 1993).
- Wolszczan, A. & Frail, D. A. A planetary system around the millisecond pulsar PSR 1257+12. *Nature* **355**, 145-147 (1992).
- Rasio, F. A., Nicholson, P. D., Shapiro, S. L. & Teukolsky, S. A. An observational test for the existence of a planetary system orbiting PSR 1257+12. *Nature* **355**, 325-326 (1992).
- Wolszczan, A. Confirmation of Earth-mass planets orbiting the millisecond pulsar PSR 1257+12. *Science* **264**, 538-542 (1994).
- Kennel, C. F. & Coroniti, F. V. in *Solar System Plasma Physics*. Vol. 2 *Magnetospheres* 105-181 (North-Holland, Amsterdam, 1979).
- Lyne, A. G. in *Pulsars: Problems and Progress* (eds Johnston, S., Walker, M. A. & Bailes, M.) 73-81 (IAU Colloquium 160, Astronomical Society of the Pacific, San Francisco, 1996).
- Tkachenko, K. Stability of vortex lattices. *Sov. Phys. JETP* **23**, 1049-1056 (1966).
- Goldstein, H. *Classical Mechanics* 205-213 (Addison-Wesley, Reading, Massachusetts, 1980).
- Weisberg, J. M., Romani, R. W. & Taylor, J. H. Evidence for geodetic spin precession in the binary pulsar 1913+16. *Astrophys. J.* **347**, 1030-1033 (1989).
- Arzoumanian, Z. *Radio Observations of Binary Pulsars: Clues to Binary Evolution and Tests of General Relativity*. Thesis, Princeton Univ. (1995).
- Cordes, J. M. in *Planets around Pulsars* (eds Phillips, J. A., Thorsett, S. E. & Kulkarni, S. R.) 43-60 (Astronomical Society of the Pacific Conference Series Vol. 36, San Francisco, 1993).
- Suleymanova, S. A. & Shitov, Y. P. Secular variations of the integrated pulse profile of, and torque on, PSR 2217+47: Precession of the neutron star? *Astrophys. J. Lett.* **422**, 17-20 (1994).

15. D'Alessandro, F. & McCulloch, P. M. Long-term timing observations of four southern pulsars. *Mon. Not. R. Astron. Soc.* **292**, 879–886 (1997).
16. Mereghetti, S. A spin-down variation in the 6 second X-ray pulsar 1E 1048.1-5937. *Astrophys. J.* **455**, 598–602 (1995).
17. Melatos, A. Bumpy spin-down of anomalous X-ray pulsars: The link with magnetars. *Astrophys. J.* **519**, L77–L80 (1999).
18. Alpar, M. A., Anderson, P. W., Pines, D. & Shaham, J. Vortex creep and the internal temperature of neutron stars. I. General theory. *Astrophys. J.* **276**, 325–334 (1984).
19. Roberts, D. H., Lehar, J. & Dreher, J. W. Time series analysis with CLEAN. I. Derivation of a spectrum. *Astron. J.* **93**, 968–989 (1987).
20. Lyne, A. G. & Graham-Smith, F. *Pulsar Astronomy* 14–22 (Cambridge, Univ. Press, 1998).

Acknowledgements

We thank D. J. Nice for providing the two-standard-profile frequency-domain fitting routine, M. Goss for obtaining the interferometric pulsar position, F. Graham Smith for reading of the manuscript and F. Camilo for discussions. I.H.S. received support from a Natural Sciences and Engineering Research Council of Canada postdoctoral fellowship.

Correspondence and requests for materials should be addressed to A.G.L. (e-mail: agl@jb.man.ac.uk).

Vortex-like excitations and the onset of superconducting phase fluctuation in underdoped $\text{La}_{2-x}\text{Sr}_x\text{CuO}_4$

Z. A. Xu*†, N. P. Ong*, Y. Wang*, T. Kakeshita‡ & S. Uchida‡

* Joseph Henry Laboratories of Physics, Princeton University, Princeton, New Jersey 08544, USA

‡ School of Frontier Sciences, University of Tokyo, Yayoi 2-11-16, Bunkyo-ku, Tokyo 113-8656, Japan

Two general features of a superconductor, which appear at the critical temperature, are the formation of an energy gap and the expulsion of magnetic flux (the Meissner effect). In underdoped copper oxides, there is strong evidence that an energy gap (the pseudogap¹) opens up at a temperature significantly higher than the critical temperature (by 100–220 K). Certain features of the pseudogap suggest that it is closely related to the gap that appears at the critical temperature (for example, the variation of the gap magnitudes around the Fermi surface and their maximum amplitudes are very similar^{2,3}). However, the Meissner effect is absent in the pseudogap state. The nature of the pseudogap state, and its relation (if any) to the superconducting state are central issues in understanding copper oxide superconductivity. Recent evidence suggests that, in the underdoped regime, the Meissner state is destroyed above the critical temperature by strong phase fluctuations^{4–7} (as opposed to a vanishing of the superfluid density). Here we report evidence for vortices (or vortex-like excitations) in $\text{La}_{2-x}\text{Sr}_x\text{CuO}_4$ at temperatures significantly above the critical temperature. A thermal gradient is applied to the sample in a magnetic field. Vortices are detected by the large transverse electric field produced as they diffuse down the gradient (the Nernst effect). We find that the Nernst signal is anomalously enhanced at temperatures as high as 150 K.

In conventional superconductors, fluctuations in the phase $\theta(r)$ of the superconducting wavefunction $\psi \exp[i\theta(r)]$ incur a sizeable cost in energy (the phase stiffness energy is large). Hence $\theta(r)$ is uniform in the absence of field and currents. In the underdoped

copper oxides, however, the small superfluid density n_s implies a small phase stiffness energy⁴. The Meissner state is readily destroyed by strong phase fluctuations. This suggests that rapidly diffusing vortices, which are highly effective in destroying phase coherence, may help to limit the critical temperature T_c . In a recent experiment, Corson *et al.*⁷ measured the complex conductivity in underdoped $\text{Bi}_2\text{Sr}_2\text{CaCu}_2\text{O}_{8+\delta}$ (BSCCO) at terahertz frequencies, and deduced a Kosterlitz–Thouless transition⁸ at T_c , with a fluctuating regime that extends about 25 K above T_c .

To detect directly the presence of vortices above T_c , we have adopted a different approach. By using a strictly d.c. probe that selectively senses vortex motion, we may detect excitations that are long-lived. An applied thermal gradient ($-\nabla T$) causes vortices to diffuse with a velocity \mathbf{v} (\mathbf{v} may be tilted relative to $-\nabla T$). The distinguishing feature of moving vortices is the Josephson electric field given by $\mathbf{E} = \mathbf{B} \times \mathbf{v}$, which reflects phase slippage caused by moving vortices. The y -component of the \mathbf{E} -field leads to a very large Nernst effect. With $-\nabla T \parallel \mathbf{x}$, the Nernst coefficient is defined as

$$\nu = E_y / (B |\nabla T|) \tag{1}$$

with the induction field $\mathbf{B} \parallel \mathbf{z}$. (Previous Nernst experiments in the copper oxides were restricted to optimally doped samples^{9–11}.) In our experiment, we measured ν versus T in five crystals of $\text{La}_{2-x}\text{Sr}_x\text{CuO}_4$ (LSCO; samples 1–5), with $0.05 < x < 0.17$, and in a crystal of Nd-doped $\text{La}_{2-y-x}\text{Nd}_y\text{Sr}_x\text{CuO}_4$ (sample N).

Figure 1 displays traces of the Nernst signal E_y versus the applied field H in sample 3 ($x = 0.10$) at temperatures between 12 and 35 K (Fig. 1a) and above 35 K (Fig. 1b). At 12 and 15 K, the behaviour

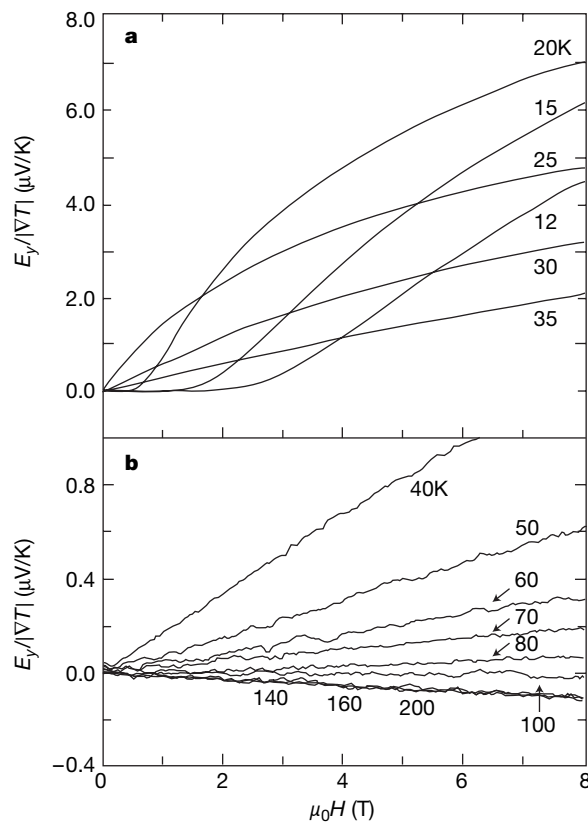


Figure 1 Nernst signals. **a**, The Nernst signal E_y (normalized to unit gradient) versus $H \parallel c$ in $\text{La}_{2-x}\text{Sr}_x\text{CuO}_4$ (sample 3, $x = 0.10$) at temperatures 12–35 K. **b**, The Nernst signal from 40 to 200 K. Above 20 K, the applied gradient is 5 K cm^{-1} , while below 20 K, it is half as large. When vortex pinning is large ($T < 25 \text{ K}$), E_y is zero over a range of $H < H_m$. Above 140 K, the curves tend asymptotically to a straight line of negative slope.

† Present address: Department of Physics, Zhejiang University, Hangzhou 310027, China.